Proceedings of ICRC 2001: 71 © Copernicus Gesellschaft 2001

ICRC 2001

On the knee in the energy spectrum of cosmic rays

J. R. Hörandel

Institut für Experimentelle Kernphysik, University of Karlsruhe, P.O. Box 3640, 76021 Karlsruhe, Germany

Abstract. The enigma of the *knee* in the cosmic–ray energy spectrum is scrutinized with an empirical model, comparing results from direct and indirect measurements. The energy spectra of individual elements, as obtained by direct observations, are extrapolated to high energies and compared to a compilation of all–particle energy spectra from air shower measurements. A model, assuming a cut-off for each species proportional to its charge Z is adopted. The fine structure of the energy spectrum with changes of the spectral index at 2.5 PeV and 300 PeV are explained by cut-offs of the proton component and of the stable elements (Z=92). The *knee* in the all–particle energy spectrum results from a charge dependent cut-off for each individual element of the galactic component. No additional cosmic ray component is required in the *knee* region to describe the observed spectrum. The model allows a prediction of the mass composition of cosmic rays at high energies, which is in agreement with experimental results from air shower experiments.

1 Introduction

The cosmic–ray energy spectrum extends over many orders of magnitude from GeV energies up to at least 10^{20} eV as a steep falling spectrum roughly following a power law $dN/dE \propto E^{-\gamma}$ with almost no special features. A closer look exhibits some fine structures, most prominent is a change in the spectral index from $\gamma_1 \approx -2.7$ to $\gamma_2 \approx -3.0$ at about 3 PeV, generally called *the knee*. Its origin is still under discussion and is generally assumed to be a corner stone in the understanding of the origin of cosmic rays.

The energy spectra of cosmic rays are measured directly up to several 10^{14} eV for individual elements with satellite and balloon–borne experiments at the top of the atmosphere. Due to the steep falling spectrum, measurements at higher energies require large detection areas or long exposure times, at present only realized in ground–based detector systems. These experiments measure extensive air showers, generated by interactions of high–energetic cosmic rays in the atmosphere.

In this work the fluxes obtained by direct measurements are extrapolated to high energies and compared to results of indirect measurements.

Correspondence to: J. R. Hörandel (joerg@ik1.fzk.de)

Theories for cosmic ray acceleration (see for example (Wiebel98) (Gaisser99)) propose acceleration processes becoming inefficient at an energy $E_C \propto Z$ where Z is the nuclear charge of the particle, and a complete cut-off is expected at higher energies, also proportional to Z. Therefore, we expect a cut-off or at least a change of the spectral index in the spectrum for the individual species at an energy E_C^Z. Inspired by these theories, we adopt an empirical model to explain the fluxes of high–energy cosmic rays.

Above about $Z \cdot 10$ GeV energy/nucleon, where the modulation due to the solar magnetic field is negligible, the energy spectra of cosmic–ray nuclei can be described by a power law. We chose the ansatz

$$\frac{d\Phi_Z}{dE}(E) = \Phi_Z^0 \cdot E^{\gamma_Z} \left[1 + \left(\frac{E}{Z \cdot E_C^p} \right)^{\epsilon} \right]^{\frac{\gamma_C - \gamma_Z}{\epsilon}} \quad , \quad (1)$$

γ_C and ϵ characterize the change in the spectrum at the cut-off energy $Z \cdot E_C^p$, with the cut-off energy E_C^p for protons.

Summing up the flux of all elements, the all–particle spectrum is obtained. We have two parameters Φ_Z^0 and γ_Z for each element and three common parameters E_C^p, γ_C, and ϵ to describe the end of the single element spectra. Φ_Z^0 and γ_Z are deduced from direct measurements of individual nuclei, the remaining 3 parameters will be derived from indirect measurements of the all–particle spectrum.

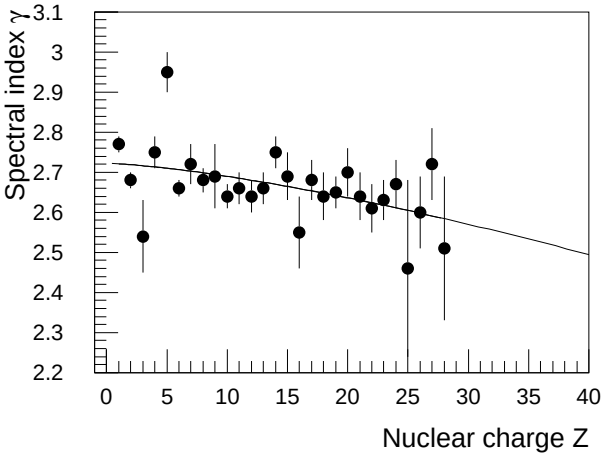

Fig. 1. Spectral indices (Wiebel98) versus nuclear charge.

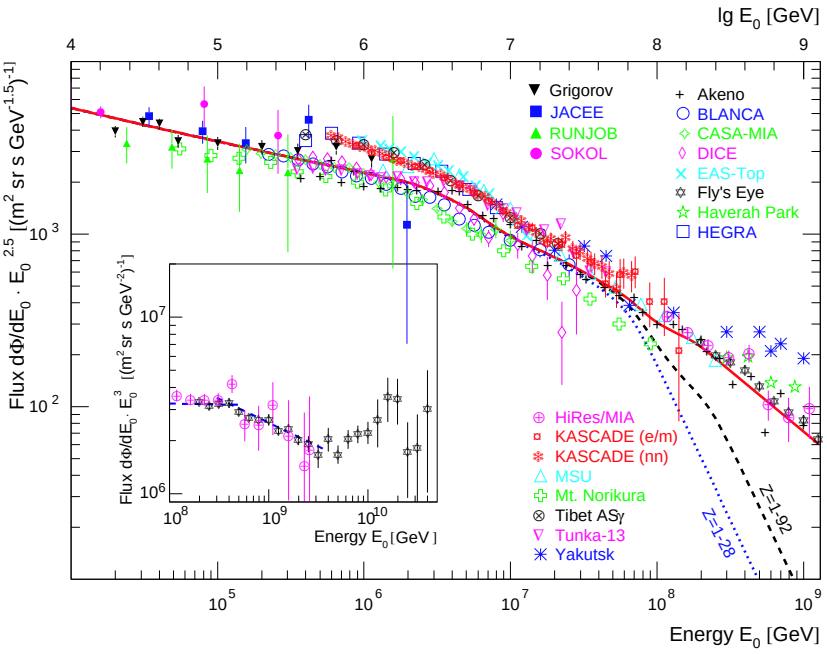

Fig. 2. All–particle energy spectrum obtained from direct observations by Grigorov (Shibata99), JACEE (Tominaga93), RUNJOB (Apanasenko98), SOKOL (Ivanenko93), and indirect measurements by AKENO (Nagano84), BLANCA (Fowler01), CASA-MIA (Glasmacher99), DICE (Swordy00), EAS-Top (Aglietta99), Fly's Eye (Bird94), Haverah Park (Lawrence91), HEGRA (Arqueros00), HiRes/MIA (Abu–Zayyad00), KASCADE parametric (electrons + muons) (Ulrich01) and neural network analysis (Roth01) (Antoni01), MSU (Fomin91), Mt. Norikura (Ito97), Tibet ASγ (Amenomori96), Tunka–13 (Gress97), and Yakutsk (Dyakonov91). The lines represent sum spectra for elements with Z=1-28 and Z=1-92. The insert shows the high–energy end of the spectrum, as measured by Fly's Eye and HiRes/MIA. The dashed line represents a fit by Bird et al. (Bird94).

2 Direct Measurements

Many direct measurements of individual nuclei have been performed using balloon–borne detectors at the top of the atmosphere and instruments on spacecrafts. A compilation by Wiebel–Sooth et al. (Wiebel98) summarizes results for energy spectra from hydrogen to nickel and gives abundance values at 1 TeV. The abundance of ultra-heavy elements ($Z > 28$) at energies just above the geomagnetic cut–off has been measured by the experiments ARIEL 6 (Fowler87) and HEAO 3 (Binns89). All stable elements of the periodic table from hydrogen up to the actinides have been found in cosmic rays. For ultra–heavy elements only the abundance is measured, no spectral information is available. Hence, the spectral indices for these elements shall be estimated.

The spectral indices for the elements from hydrogen to nickel, taken from (Wiebel98), are shown in figure 1 versus the nuclear charge. Theories using a nonlinear model of Fermi acceleration in supernovae remnants predict a more efficient acceleration for elements with large mass to charge ratios compared to elements with a smaller A/Z ratio, see for example (Ellison93). Consequently, it is expected that elements with higher A/Z have a flatter spectrum. Such a trend is visible in figure 1.

In our model we assume the relation $\gamma(Z) = A + B \cdot Z^C$ to describe the Z dependence of the spectral indices. The three parameters are determined by fits to the values in figure 1 as well as to the all–particle spectrum as described below. The curve in figure 1 represents the best fit, exhibiting a decreasing spectral index with the nuclear charge:

$$\gamma(Z) = 2.72 - 0.130 \cdot 10^{-2} \cdot Z^{1.4} \quad . \tag{2}$$

This expression is applied to estimate the spectral indices for ultra–heavy elements ($Z > 28$) in order to extrapolate the flux obtained by ARIEL 6 and HEAO 3.

Even if the abundance of ultra–heavy elements is small at low energies, their relative number will increase due to their assumed flatter energy spectrum. In our model they become more and more important for the all–particle spectrum at high energies, since all lighter elements have already reached their cut-off energy $E_C^Z \propto Z$.

3 Indirect Measurements

Many groups published results on the all–particle energy spectrum from indirect measurements, recent results are compiled in figure 2. The overall agreement between the experiments is quite good, the differential fluxes multiplied by $E^{2.5}$ agree within a factor of two.

Typical uncertainties of air shower experiments in the absolute energy calibration are quoted to be in the order of 10% to 20%. The spectra can be normalized by slightly changing the energy scale in order to fit the flux given by direct measurements around 10^5 GeV. The result is presented in figure 3 together with the normalization factors. They are in agreement with the above quoted energy uncertainties. The mean normalization factor is $-5.4\% \pm 1.5\%$, i.e. most experiments slightly overestimate the primary energy. A fact which could exhibit a systematic effect in the hadronic interaction models used to interpret the air shower data. The similar shape obtained by the different experiments is obvious in this representation, an interesting observation, since the energy scaling does not change the shape of the spectra.

A *knee* at about 3 PeV is clearly visible in the figure. Assuming this bend is caused by the cut-off of the proton com-

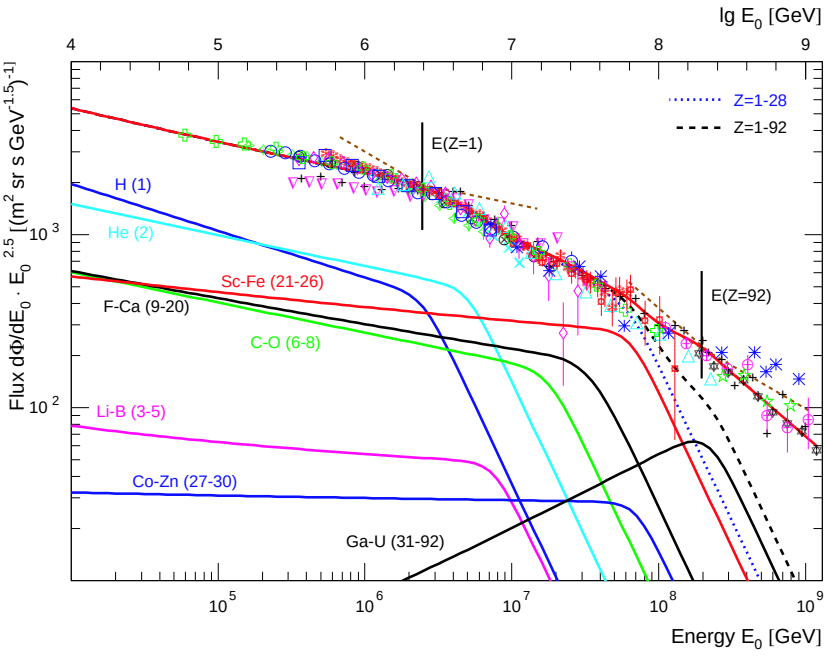

Fig. 3. Normalized all–particle energy spectrum. The normalization factors for the energy scales are:

Experiment	Norm. Factor
AKENO	0%
BLANCA	2%
CASA–MIA	2%
DICE	0%
EAS–Top	−13%
Fly's Eye	−5%
Haverah Park	−9%
HEGRA	−11%
HiRes	−5%
KASCADE (e/m)	−9%
KASCADE (nn)	−9%
MSU	−9%
Mt. Norikura	8%
Tibet	−11%
Tunka–13	−7%
Yakutsk	−10%

The solid curves (H to Ga-U) represent extrapolated spectra for groups of elements according to our assumptions.

ponent, the galactic component should extend up to about $92 \cdot 3$ PeV≈ 0.3 EeV. A change in the spectral slope around 3 to $4 \cdot 10^8$ GeV is visible in figure 2, especially in the insert — the dashed line represents a fit taken from (Bird94). This observation is confirmed by results from AKENO and Haverah Park (Bird94). The change in slope coincidences well with the proposed cut-off of the heaviest nuclei of the galactic component.

4 All–Particle Energy Spectrum

The parameters E_C^p, ϵ, and γ_C are determined from indirect measurements using the data as presented in figure 3. A least–square fit to the all–particle spectrum, using the parameters Φ_Z^0 and γ_Z for elements up to nickel results in the blue, dotted graph in figure 3. The parameters describing the shape of the cut-off for the individual element spectra are $\epsilon = 7$ and $\gamma_C = 4.3$. The proton *knee* is found to be at $E_C^p = 2.5$ PeV.

Next, the coefficients for the $\gamma(Z)$ dependence shall be determined. The values influence the all–particle spectrum and must fit the values in figure 1. A combined fit of figure 1 and the all–particle spectrum yields the coefficients in equation 2. The resulting sum spectrum for elements with Z=1 to 92 is plotted in figure 3 as dashed curve. The contribution of ultra–heavy elements causes a change in the spectral index around 0.3 EeV, as has been observed by the Fly's Eye and HiRes experiments.

Above this energy, a new (extragalactic) component takes over and dominates the spectrum at the highest energies. This component is introduced into the model *ad hoc*, adding the required flux to the galactic component to match the measured flux values. This flux difference as function of energy is needed to calculate the mass composition in the next section. The resulting all–particle spectrum, including the *ad hoc* component is shown as a red, solid curve in figures 2 and 3. One notices that the empirical model consistently describes the cosmic–ray energy spectrum from several 10 GeV up to 10^9 GeV.

5 Mass Composition

All parameters in equation 1 being defined, the spectrum for each species can be deduced. To avoid confusion, only the spectra of groups of elements are shown in figure 3.

It is now possible to calculate the mass composition of cosmic rays for a given energy using for example the mean logarithmic mass, defined as

$$\langle \ln A \rangle = \sum_i r_i \ln A_i \qquad (3)$$

where r_i is the relative fraction of component i with mass A_i. One difficulty in deriving a value for $\langle \ln A \rangle$ is the unknown composition of the "extragalactic component" which has been introduced *ad hoc* to describe the observed all–particle spectrum. Several theories predict an extragalactic component consisting of proton and helium nuclei only, see for example (Biermann93). We, therefore, assume a mixture of protons and helium. The predicted mean logarithmic mass is presented in figure 4 as function of the particle energy. The values for the galactic component increase up to pure uranium, since all other species already reached their cut-off energies (dotted, red line). Assuming pure protons and pure helium nuclei for the extragalactic component, the dashed, red lines are obtained, respectively.

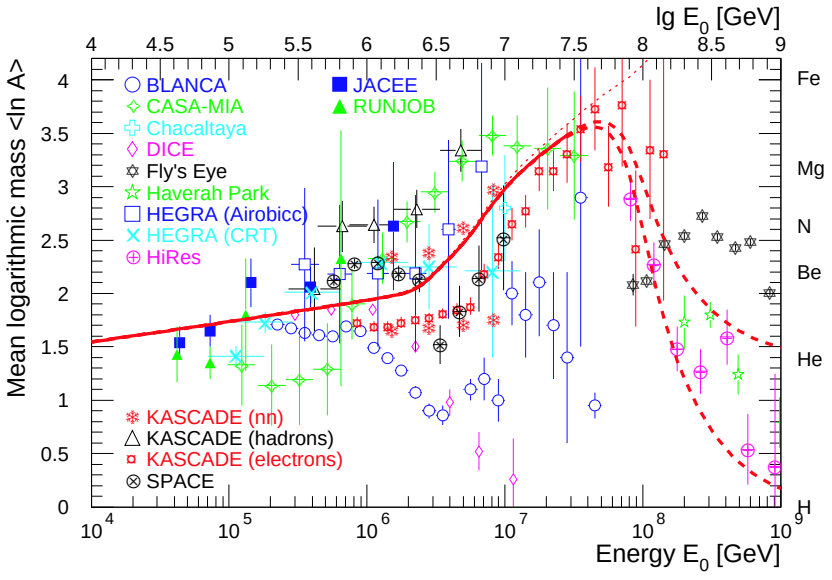

Fig. 4. Mean logarithmic mass vs. particle energy from JACEE, RUNJOB (Shibata99); CASA–MIA (Glasmacher99); Chacaltaya (Aguirre00); DICE (Swordy00); Haverah Park (Watson00); HEGRA Airobicc (Arqueros00), CRT (Bernlöhr98); HiRes (Abu–Zayyad00); KASCADE neural network (two extreme results from different observables) (Roth01) (Antoni01), parametric analysis using electrons + muons (Ulrich01), hadrons + muons (Hörandel98); BLANCA, Fly's Eye, and SPACE taken from (Fowler01) with QGSJET interpretation. Some papers quote results for several interaction models used to interpret the data, in such a case only QGSJET results are shown. The curves show the mass function according to the empirical model.

In the figure the calculated $\langle \ln A \rangle$ values are compared with results from several experiments. The measurements exhibit a wide scattering of the $\langle \ln A \rangle$ values, which is mainly caused by different interpretations of the data due to uncertainties in the interaction models used. Different models lead to different mass compositions for the same measurement and the same interaction model leads to different values of $\langle \ln A \rangle$ for different observables. For example, KASCADE uses several models and observables and obtains different results (Hörandel98) (Antoni01). Two extreme results in a neural network analysis when using different observables (Antoni01) are shown in the figure to illustrate the effect.

Despite of the discrepancies in the measurements or their interpretation, the general trend of the predicted mass function is supported by most experiments.

6 Conclusion

Adopting an empirical model with a cut-off for individual element spectra at an energy $E_C^Z = Z \cdot E_C^p$, and extrapolating the energy spectra of individual nuclei obtained by direct measurements to high energies, the energy spectrum of cosmic rays in the range from 10 GeV up to almost 1 EeV can be described consistently, and the fine structure of the spectrum can be explained. The all–particle energy spectrum compiled from many air shower experiments shows two changes in spectral slope at $E_C^p = 2.5$ PeV and 0.3 EeV ($\approx 92 \cdot E_C^p$), which can be correlated to the cut–off energies of protons (Z=1) and the heaviest stable nuclei (Z=92). Within the model ultra–heavy nuclei (Z=30-92) with spectral indices $\gamma(Z) \propto Z^{1.4}$ are important to describe the energy spectrum around 100 PeV. The predicted mass composition is in agreement with results from air shower experiments.

Acknowledgements. The author would like to thank Joachim Engler and Karl–Heinz Kampert for helpful comments on this work.

References

Abu–Zayyad, T. et al., 2000, astro-ph/0010652
Aglietta, M. et al., 1999, Astropart. Phys. **10**, 1
Aguirre, C. et al., 2000, Phys. Rev. D **62**, 032003
Amenomori, M. et al., 1996, Ap. J. **461**, 408
Antoni, T. et al., 2001, accepted by Astropart. Phys.
A.V. Apanasenko et al., 1998, ISAS–report No. 37
Arqueros, F. et al., 2000, Astron. Astrophys. **359**, 682
Bernlöhr, K, et al., 1998, Astropart. Phys. **8**, 253
Biermann, B.L., 1993, Astron. Astrophys. **271**, 649
Binns, W.R. et al., 1989, Ap. J. **346**, 997
Bird, D.J. et al., 1994, Ap. J. **424**, 491
Dyakonov, M.N. et al., 1991, Proc. 22^{nd} ICRC, Dublin **2**, 93
Ellison, D.C., 1993, Proc. 23^{rd} ICRC, Calgary **2**, 219
Fomin, Y.A. et al., 1991, Proc. 22^{nd} ICRC, Dublin **2**, 85
Fowler, P.H. et al., 1987, Ap. J. **314**, 739
Fowler, J.W. et al., 2001, Astropart. Phys. **15**, 49
Gaisser, T.K., 1999, Cosmic Rays and Particle Physics, Cambridge
Glasmacher, M.A.K. et al., 1999, Astropart. Phys. **10**, 291
Gress, O.A. et al., 1997, Proc. 25^{th} ICRC, Durban **4**, 129
Hörandel, J.R. et al., 1998, Proc. 16^{th} ECRS, Alcala, 579; and Engler, J. et al., 1999, Proc. 26^{th} ICRC, Salt Lake City **1**, 349
Ito, N. et al., 1997, Proc. 25^{th} ICRC, Durban **4**, 117
I.P. Ivanenko et al., 1993, Proc. $23rd$ ICRC, Calgary **2**, 17
Lawrence, M.A. et al., 1991, J. Phys. G: Nucl. Part. Phys. **17**, 733
Nagano, M. et al., 1984, J. Phys. G: Nucl. Part. Phys. **10**, 1295
Roth, M. et al., 2001, Proc. 27^{th} ICRC, Hamburg
Shibata T., 1999, Nucl. Phys. B (Proc. Suppl.) **75A**, 22
Swordy, S.P., Kieda, D.B., 2000, Astropart. Phys. **13**, 137
Tominaga, T. et al., 1993, Proc. 23^{rd} ICRC, Calgary **2**, 21
Ulrich, H. et al., 2001, Proc. 27^{th} ICRC, Hamburg
Watson, A.A., 2000, Physics Reports **333-334**, 309
Wiebel–Soth, B. et al., 1998, Astron. Astroph. **330** , 389